Voltage-sensitive and solvent-sensitive processes in ion channel gating
Kinetic effects of hyperosmolar media on activation and deactivation of sodium channels

M. D. Rayner, J. G. Starkus, P. C. Ruben, and D. A. Alicata

Pacific Biomedical Research Center, Békésy Laboratory of Neurobiology, Honolulu, Hawaii 96822; and Department of Physiology, John A. Burns School of Medicine, University of Hawaii, Honolulu, Hawaii 96822 USA

ABSTRACT   Kinetic effects of osmotic stress on sodium ionic and gating currents have been studied in crayfish giant axons after removal of fast inactivation with chloramine-T. Internal perfusion with media made hyperosmolar by addition of formamide or sucrose, reduces peak sodium current (before and after removal of fast inactivation with chloramine-T), increases the half-time for activation, but has no effect on tail current deactivation rate(s). Kinetics of ON and OFF gating currents are not affected by osmotic stress. These results confirm (and extend to sodium channels) the separation of channel gating mechanisms into voltage-sensitive and solvent-sensitive processes recently proposed by Zimmerberg J., F. Bezanilla, and V. A. Parsegian. (1990. Biophys. J. 57:1049–1064) for potassium delayed rectifier channels. Additionally, the kinetic effects produced by hyperosmolar media seem qualitatively similar to the kinetic effects of heavy water substitution in crayfish axons (Alicata, D. A., M. D. Rayner, and J. G. Starkus. 1990. Biophys. J. 57:745–758). However, our observations are incompatible with models in which voltage-sensitive and solvent-sensitive gating processes are presumed to be either (a) strictly sequential or, (b) parallel and independent. We introduce a variant of the parallel model which includes explicit coupling between voltage-sensitive and solvent-sensitive processes. Simulations of this model, in which the total coupling energy is as small as 1/10th of kT, demonstrate the characteristic kinetic changes noted in our data.

INTRODUCTION

The effects of D_2O on sodium ionic and gating current kinetics in Myxicola giant axons (Schauf and Bullock, 1979, 1980, 1982) indicated two principal conclusions: (a) the major voltage-sensitive transitions of primary activation precede a final D_2O-sensitive transition into the open state however, (b) sodium channels leave the open state (during tail current deactivation) via a solvent-insensitive pathway. Alicata et al. (1990) confirmed the previous results of Schauf and Bullock, noting additionally that secondary activation kinetics (after a brief return to holding potential), like deactivation kinetics, are solvent insensitive. These observations are incompatible with the predictions of linear sequential models for the activation/deactivation mechanism. Sodium channels apparently activate via two alternative routes, a solvent-sensitive path or a solvent-insensitive path, depending on initial conditions.

Zimmerberg et al. (1990) provided additional evidence suggesting that channel gating involves separable voltage-sensitive and solvent-sensitive mechanisms. Increasing osmotic stress decreased macroscopic potassium conductance in squid axon delayed rectifier channels, suggesting that the probability of channel opening decreased in proportion to the osmotic strength of the bathing solution. Furthermore the effect of osmolarity was independent of test potential. They concluded that: (a) the conducting pathway cannot open until some part of the channel structure has been hydrated; (b) the region hydrated must be effectively inaccessible to solutes; (c) no significant net charge movement is involved in the channel hydration process.

The present study was undertaken first, to determine whether sodium channels are affected by osmotic stress in a similar manner to the delayed rectifier potassium channels studied by Zimmerberg et al. (1990), second, to compare the kinetic effects of osmotic stress and D_2O (see Alicata et al., 1990) and, finally, to further clarify the functional relationship between voltage-sensitive and solvent-sensitive components of sodium channel gating. Our results extend the findings of Zimmerberg et al. (1990) to sodium channels and confirm that D_2O and hyperosmolar media have similar qualitative effects on sodium channel kinetics. These data further indicate that voltage-sensitive and solvent-sensitive gating mechanisms must be coupled, such that gating charge movements necessarily precede (and presumably trigger) solvent-sensitive changes in channel hydration during both activating (depolarizing) and deactivating (repolarizing) voltage steps.

These results have been presented in abstract form (Starkus et al., 1991; Rayner and Starkus, 1991).

Address correspondence to Dr. Martin D. Rayner, University of Hawaii, Pacific Biomedical Research Center, Békésy Laboratory of Neurobiology, 1993 East West Road, Honolulu, HI 96822.

METHODS

Crayfish medial giant axons were dissected free, internally perfused and voltage clamped following methods initiated by Shrager (1974) and modified as described by Starkus et al. (1984) and Heggeness and Starkus (1986). Pulse generation and data recording methods used here were as described by Rayner and Starkus (1989) and Alicata et al. (1989, 1990). Axons were maintained between 6 and 8°C; potassium currents were blocked by perfusion with solutions containing Cs or tetramethylammonium[1] (TMA) ions (see below); sodium currents were blocked as necessary to permit recording of gating currents by adding 100 nM tetrodotoxin (TTX) to the external perfusate; fast inactivation was removed using chloramine-T (Sigma Chemical Co., St Louis, MO) following the procedure described by Alicata et al. (1990); internal solutions were made hyperosmolar by addition of sucrose or by partial substitution of water with formamide (see below); osmolarities were checked before perfusion was initiated. In preliminary experiments we found no significant qualitative differences between results obtained when hyperosmolar media were added to both sides of the membrane or perfused only internally. However, axon survival was consistently reduced when the external perfusate was markedly hyperosmolar (see also Alicata et al., 1989; Alicata et al., 1990). In this study, therefore, unlike the work of Zimmerberg et al. (1990) where their strictly quantitative approach required simultaneous exposure of both membrane surfaces to media of identical osmolarity, we changed only the internal perfusate. Specific aspects of the methods used for this study are considered in more detail below.

Series resistance compensation

Zimmerberg et al. (1990) show that their steady-state measurements of osmotically induced changes in limiting conductance are not markedly affected by possible changes in series resistance (R_s). They note that small effects of external medium conductivity could be fully compensated by assuming associated changes in R_s. Additionally, R_s may be altered if external perfusate osmolarity affects Schwann cell volume, thus either widening or constricting the tubules crossing the Schwann cell layer (see Shrager et al., 1983). However, where only internal osmolarity is changed, R_s changes will primarily reflect changes in volume of the Frankenhaeuser-Hodgkin space resulting from maintained water fluxes across the axolemma. Such changes in R_s have been shown to affect clamp rise time in both squid (Stimers et al., 1987) and crayfish axons (Alicata et al., 1989), in both cases with consequent effects on gating current waveforms.

In this study, series resistance compensation was initially set to 10 ohm·cm² and then fine-tuned (within the range 9–12 ohm·cm²) by comparing kinetics of sodium currents at 0 mV test potential, from holding potentials of −120 and −85 mV. Compensation was adjusted during the control period in isosmolar perfusate, until we could detect no kinetic effects of the greater than twofold change in current magnitude produced by this shift in holding potential. Thereafter, during hyperosmolar perfusion, we followed the method introduced by Alicata et al. (1989) to correct for osmotically induced R_s changes. Monitoring peak capacity current in voltage steps at very negative potentials (from −150 to −200 mV for 4 ms), R_s adjustments were made as needed to maintain constant peak capacity current (after subtraction of linear leakage current) and hence constant clamp rise time. Readjustment of R_s compensation using the peak capacity current method is essential for comparison of gating currents after introduction of hyperosmolar perfusates because this is the only

method for assessing changes in R_s after block of ionic currents and while maintaining voltage clamp. This method also provides a convenient and rapid method for monitoring (and correcting) R_s compensation during sodium current recording.

Peak capacity current was carefully readjusted to its control level after change to a hyperosmolar perfusate. We continued to monitor peak capacity current at ~5 min intervals for the remainder of the experiment, readjusting R_s compensation as necessary. For an increase in internal osmolarity from 0.44 (the control level in crayfish axons) to 0.89 osmol/kg, it was typically necessary to increase R_s compensation to ~15 ohm·cm² over the first 10 min, with further small adjustments over the next 20 min. Although we noted marked increases in leak conductance after washout of hyperosmolar perfusates (see also Zimmerberg et al., 1990), we found it necessary to return R_s compensation to ~10 ohm·cm² during washout to prevent ringing of the clamp and to maintain (leak subtracted) peak capacity current at its initial control level.

Filtering

No analogue filtering was used in this study, although the digitization sampling interval effectively limits inputs at frequencies > 1 mHz (for 1 μs sample intervals) or 500 kHz (for 2 μs intervals). Unfiltered data traces were recorded directly on hard disk. These traces were smoothed before analysis, using a discrete fourier transform smoothing routine, modified from the description of Ludeman (1986) to include adjustable window length and progressive tapering of the windows at the ends of the filtered region. Digital filtering was applied according to the following criteria: for the first 50 μs after the start of a voltage step, no filtering; the next 50 μs was filtered at 100 kHz; the next 100 μs, at 50 kHz; the remainder of the record, at 10 kHz. Where multiple voltage steps were imposed during a single trace, this sequence was restarted for each voltage step. Overlay of smoothed and unfiltered traces showed no detectable time shifts or kinetic distortions introduced by this procedure.

Solutions

All experiments were carried out using low Na external solutions to maintain peak sodium current at less than 1.5 mA/cm² under control conditions. The external perfusate contained (in millimolar): 75 Na, 13.5 Ca, 2.6 Mg, 135 TMA, 242.2 Cl, 2 Hepes; adjusted to pH 7.55. Internal perfusates contained (in millimolar): 0 Na, 0 K, 230 Cs, 60 F, 170 Glutamate, 1 Hepes; adjusted to pH 7.35. Osmolarity of these control solutions was 0.43–0.44 osmol/kg. Hyperosmolar formamide solutions were made immediately before use by substitution of Formamide (Sigma Chemical Co., St Louis, MO) for 5 ml or 10 ml of water in 100 ml of internal perfusate. Hyperosmolar sucrose solutions were made by addition of sucrose (Alfa Products, Danvers, MA) to the control internal perfusate. Osmolarity of all test solutions was checked by freezing point osmometer immediately before use. Corrections were made for an electrode junction potential of 8–10 mV and this junction potential changed by <1 mV during exposure to hyperosmolar perfusates. Electrode drift did not exceed 2–3 mV in these experiments.

Computer simulations

Simulations were carried out using a Sun 3/60 computer (Sun Microsystems, El Segundo, CA). Our modeling program employs simple Euler integration to solve the array of simultaneous equations representing the allowed transitions within each particular model formulation. Cumulative errors were <0.001% at the end of each model run. All voltage steps were presumed to be instantaneous.

---

[1]*Abbreviations used in this paper:* TMA, tetramethylammonium; TTX, tetrodotoxin; VDAC, voltage dependent anion channel.

Holding potential was set to −120 mV for each simulation and calculated initial state occupancies were used for each model run. Models were simulated in "pronased" form (i.e., without fast inactivation). See Appendix for further information on modeling strategies.

RESULTS

Effects of hyperosmolar perfusates in axons with intact fast inactivation

After a control period in isosmolar perfusate (∼0.45 osmol/kg), axons were perfused internally with solutions made hyperosmolar either by addition of sucrose or by partial substitution of the ionizing solvent, formamide. Axons were then carefully recompensated for increase in R_s resulting from the change in osmolarity of the internal perfusate (see Methods).

Fig. 1 demonstrates the effects of hyperosmolar perfusates on sodium channel kinetics in axons with intact fast inactivation. The pulse protocol used here was intro-

duced by Oxford (1981) to study the reversibility of the activation process. A depolarizing voltage step (here from −120 to 0 mV) is interrupted by a brief (50 μs) return to holding potential, followed by a second, equal, depolarizing step. Oxford (1981) reasoned that the relatively fast "secondary activation," occurring during the second depolarizing step, indicated that channels did not have time to return to their resting condition during a brief return to holding potential. Alicata et al. (1990) used this protocol to demonstrate that, despite the D_2O-sensitivity of primary activation, neither fast deactivation nor secondary activation were detectably D_2O-sensitive.

Fig. 1, A–C, shows records for this pulse sequence obtained before (trace a) and during (trace b) exposure to hyperosmolar 0.5 M sucrose solution (∼0.9 osmol/kg). Fig. 1 A shows the unscaled records where the suppression of maximum conductance in hyperosmolar perfusate is directly visible. In Fig. 1, B and C, to
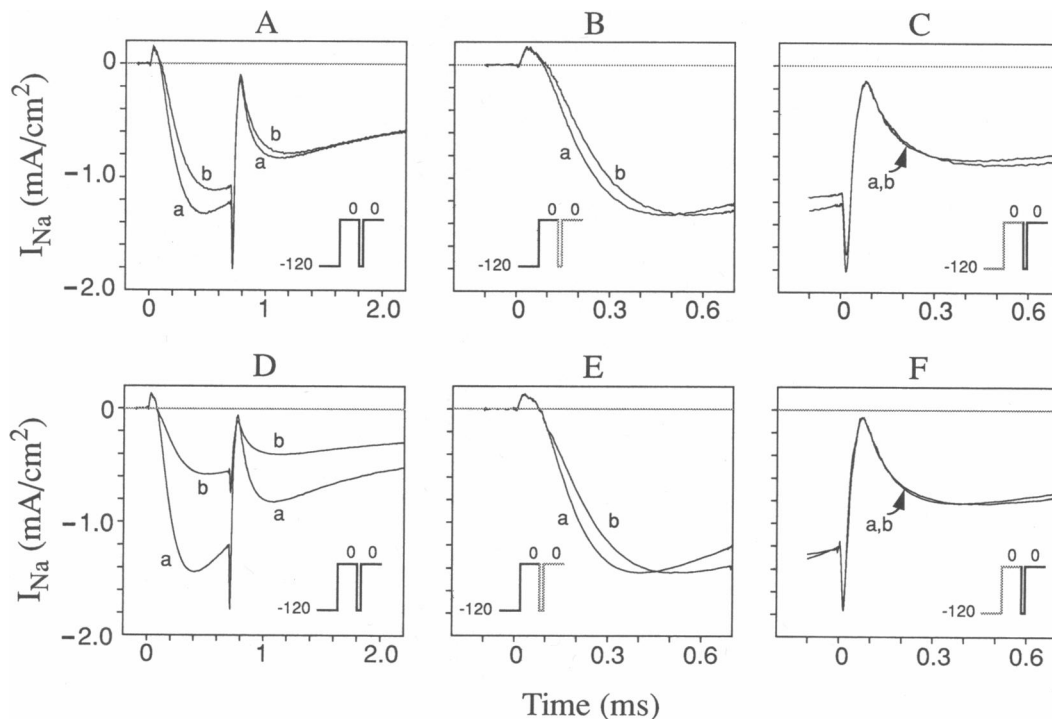

FIGURE 1 Effects of internal perfusion with hyperosmolar solutions on inward sodium current in axons with intact fast inactivation. A–C records in control and 0.5 M sucrose internal perfusates; D–F records in control and 10% formamide. (A) Effects of 0.5 M sucrose perfusate (trace b) compared with isosmolar control (trace a), during a step from −120 mV holding potential to 0 mV test potential. After 0.7 ms at 0 mV, command potential was shifted back to −120 mV for 50 μs before return to 0 mV (see pulse pattern insert). (B) Effect of 0.5 M sucrose perfusate on primary activation kinetics. Same traces as in A shown on expanded time base but including only the initial depolarization (solid line in pulse pattern insert). Trace b has been scaled to control peak magnitude (trace a) to demonstrate kinetic changes during the rising phase of primary activation. (C) Effect of 0.5 M sucrose perfusate on fast deactivation and secondary activation kinetics. Traces correspond to voltage steps indicated by solid line in pulse pattern insert. Trace b has been rescaled to match control current (trace a) just before the secondary activation step. (D–F) Equivalent data from a different axon exposed to 10% formamide perfusate. Data for A–C from axon 900801. Data for D–F from axon 900726. See Methods for solution information.

facilitate kinetic comparisons between these records, trace *b* has been scaled to control peak magnitude and the time base expanded. Fig. 1 *B* shows the primary activation step to 0 mV for both control and 0.5 M sucrose traces. The hyperosmolar sucrose perfusate increased the half-time for channel activation from 182 to 213 μs and slowed τ_h from 2.15 to 2.48 ms (as determined from single pulse traces, not shown). Fig. 1 *C* shows the rapid tail currents associated with the brief return to holding potential, followed by secondary activation of the sodium channels during the return step to 0 mV. Neither the fast tail current kinetics nor the secondary activation kinetics appear detectable affected by the hyperosmolar sucrose perfusate.

Fig. 1, *D–F*, show equivalent records from a different axon before (trace *a*) and during (trace *b*) internal perfusion with 10% formamide solution (~2.9 osmol/kg). Fig. 1 *D* here shows the unscaled records where the larger suppression of peak conductance from the higher osmolarity perfusate is readily apparent. Fig. 1 *E* again shows the records for the primary activation step scaled to equal peak magnitude. Fast inactivation was slowed (τ_h increased from 1.87 to 2.66 ms) and the half-activation time increased from 168 to 197 μs. However, Fig. 1 *F* again shows no significant change in the secondary activation rate.

Bearing in mind our previous finding that hyperosmolar formamide does not affect the kinetics of IgON (Alicata et al., 1989), the kinetic effects of these hyperosmolar perfusates follow the same pattern shown for solvent substitution with D_2O (see Alicata et al., 1990). On the other hand the conditions used here are not ideal for more detailed investigation of the effects of osmotic stress. The presence of fast inactivation makes suspect any quantitative study of the suppression of peak conduc-

tance. Furthermore, in Fig. 1 *C*, and *F*, assessment of secondary activation rate is complicated by the differences in fast inactivation rate which are also apparent in these records. Fast inactivation was therefore removed using chloramine-T (Wang et al., 1985) in the remainder of the work presented here.

Effects of hyperosmolar perfusates after removal of fast inactivation

Fig. 2 demonstrates the effects of hyperosmolar sucrose media on sodium channel activation and deactivation. In axons pretreated with chloramine-T, as Hahin (1988) has pointed out, removal of fast inactivation also removes the effect of prepulse duration on tail current kinetics. Fig. 2 *A* shows activation and deactivation before (trace *a*) and after (trace *b*) exposure to hyperosmolar sucrose solution (0.9 osmol/kg). Note both the reduction in peak current and the slowing of activation by hyperosmolar media (cf. Fig. 1) in these unscaled records. Nevertheless, the tail currents appear identical in this slow time-base record. The same tail current records are compared, using a faster time base, in Fig. 2 *B*. Whereas neither the fast nor the slower kinetic components of these tail currents are slowed by hyperosmolar sucrose, it is apparent that the peak of the fast tail current is smaller in hyperosmolar perfusate (trace *b*), in proportion to the reduced peak inward current at 0 mV. Hence, when the sucrose record is scaled to control peak current magnitude (see Fig. 2 *C*), the intercept of the scaled slow tail component appears larger during sucrose perfusion (Fig. 2 *C*, trace *b*). We found that tail currents before and after sucrose are best fitted by the sum of three exponential terms. However, there are no significant differences between the time constants for
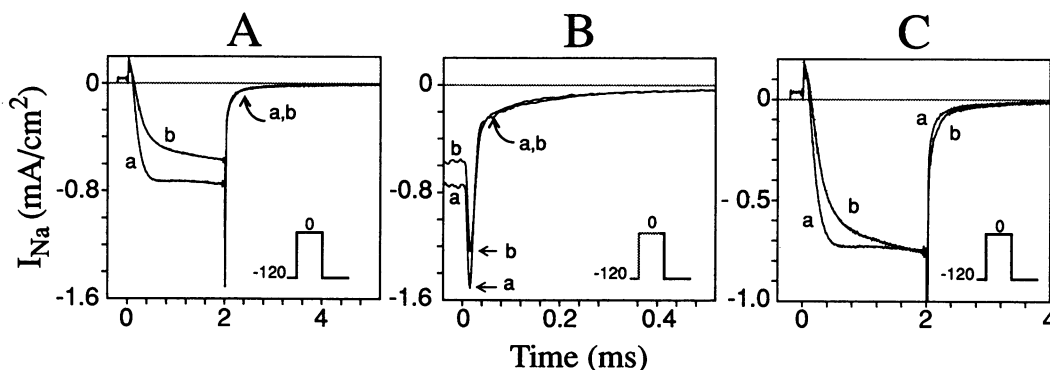

FIGURE 2 Effects of internal hyperosmolar sucrose (0.9 osmol/kg) on primary activation and tail current deactivation in an axon pretreated with 10 mM chloramine-T. Traces *a* in isosmolar control perfusate; traces *b* in hyperosmolar perfusate. (*A*) Unscaled records showing primary activation and deactivation. Note slow time base of these records. Holding potential was −120 mV. Test pulse to 0 mV for 2 ms. (*B*) Tail currents from *A* on an expanded time base. (*C*) Records from *A* with trace *b* rescaled to match isosmolar control record at 2 ms. All data from axon 900829.
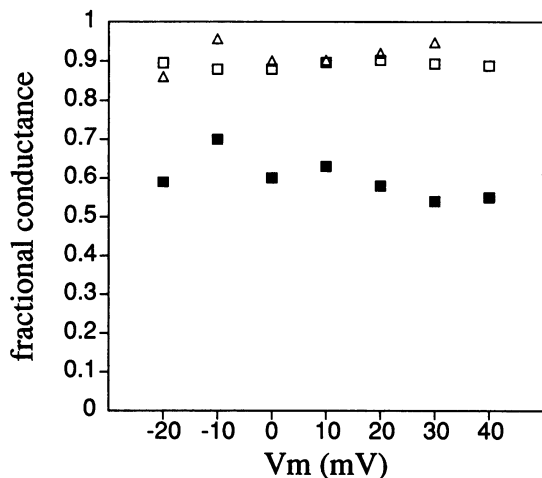
FIGURE 3 Fractional conductance remains constant across voltage in two axons exposed to 0.5 M sucrose perfusate (*open symbols*) and one axon perfused with 1 M sucrose medium (*solid squares*). Conductance ratios calculated from peak sodium conductances before and during exposure to hyperosmolar perfusate, in axons corrected for series resistance changes using the peak capacity current method (see Methods). (*Open squares*) axon 910206; (*open triangles*) axon 910206B; (*solid squares*) axon 910130.

these relaxations before and after sucrose exposure. The only consistent effect of sucrose perfusion is to increase the relative intercepts of the two slower exponential components (see Figs. 2, *B* and *C*).

Figs. 3 and 4 explore the voltage sensitivity of the solvent-sensitive process by two different approaches in axons pretreated with chloramine-T. Fig. 3 examines the suppression of peak conductance by hyperosmolar solutions at different test potentials, whereas Fig. 4 evaluates the effects of hyperosmolar solutions on ON and OFF gating currents. Fig. 3 presents peak conductance ratios (hyperosmolar peak conductance/control peak) from two axons in 0.9 osmol/kg perfusate (open symbols) and one axon in 1.3 osmol/kg perfusate (solid circles) across the voltage range from −20 to 40 mV. No significant voltage-sensitivity is apparent in these data.

Fig. 4 shows the lack of effect of a twofold increase in internal perfusate osmolarity on gating current kinetics. The data presented here are from three different axons within the series of 10 axons in which similar results were obtained. Fig. 4 *A* shows two records of ON gating currents in a step from −120 mV holding potential to 0 mV, obtained in control perfusate (trace *a*, 0.45 osmol/ kg) and during exposure to hyperosmolar sucrose solution (trace *b*, 0.9 osmol/kg). Fig. 4 *B* shows the OFF gating currents for the return step from 0 to −120 mV. In neither instance is there any detectable effect on gating current kinetics. Finally, in Fig. 4 *C*, we demonstrate that the secondary activation seen after a 50 μs return to holding potential is also unaffected by hyperosmolar sucrose. The lack of effect on gating current kinetics shown in these records is a readily repeatable observation provided that sufficient care is taken in readjusting R_s compensation against the independent criterion of peak capacity current (see Methods). For
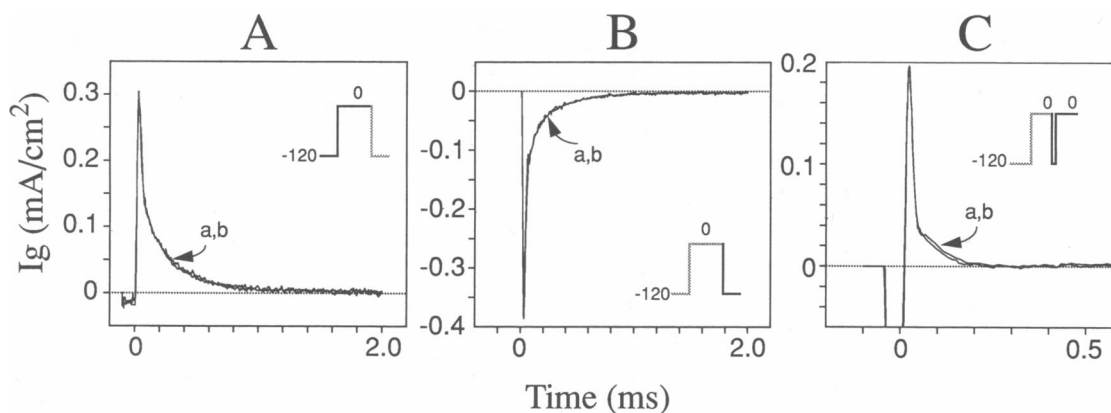

FIGURE 4 Lack of effect of hyperosmolar sucrose perfusate (0.9 osmol/kg) on gating currents. Control records (*traces a*) in isosmolar internal perfusate are compared with records taken after 20 to 30 min exposure to sucrose perfusate (*traces b*). Axons pretreated with 10 mM chloramine-T to remove fast inactivation. Sodium currents blocked by addition of 100 nM TTX to external perfusate. (*A*) ON gating currents during primary activation after a voltage step to 0 mV. Data from axon 900827. (*B*) OFF gating currents during repolarization to −120 mV. Data from axon 900830. (*C*) ON gating currents during secondary activation after a 50 μs return to −120 mV. Note expanded time base in these records, also clipping of the peak IgOFF generated during the brief return to holding potential. Data from axon 900815. Records obtained in hyperosmolar media were scaled by 15 to 20% to correct for rundown.

example, in the experiment of Fig. $4A$, R_s compensation was increased from 12 ohm·cm^2 in control conditions to 14 ohm·cm^2 on initial exposure to hyperosmolar perfusate and then progressively further increased to 16.8 ohm·cm^2 at ~30 min after exposure to the hyperosmolar sucrose solution. During washout R_s compensation was returned to 12 ohm·cm^2, to again match control peak capacity current. Unfortunately, the increased leakiness of axons after return from hyperosmolar to control perfusates (noted also by Zimmerberg et al., 1990) made it difficult to collect reliable gating currents during the washout period. Nevertheless, these results provide clear evidence to indicate that voltage-sensitive gating charge displacements are inherently insensitive to solvent changes.

We next return to a more thorough examination of the effects of hyperosmolar solutions on secondary activation kinetics after removal of fast inactivation with chloramine-T. Fig. 5 demonstrates the effects of hyperosmolar sucrose solutions (0.9 osmol/kg) on secondary activation at two different interpulse intervals (50 and 400 μs). In both Fig. 5, A and B, it is again clear that primary activation is slowed: compare trace a_1, the control record, with trace b_1 after exposure to the hyperosmolar medium. The half activation times are 238, 302 μs for traces a_1 and b_1, respectively. Trace b_1 was scaled to peak magnitude of the control prepulse sodium current to facilitate visual comparison of these activation rates. In contrast to the evident slowing of primary

activation, neither the fast component of tail current nor the rapid secondary activation seen after a 50 μs return to holding potential are noticeably affected (Fig. $5A$) by sucrose perfusion (compare traces a_2 and b_2 in Fig. $5A$). In Fig. $5B$, after a longer (400 μs) return to holding potential, it is apparent that the slower components of the tail currents (which become visible during the longer interpulse interval) show the same change of intercept made evident in Fig. $2C$ by scaling the sucrose records to control prepulse magnitude. Furthermore, where this indirect evidence of solvent sensitivity becomes detectable in the tail current rates, the subsequent secondary activation also shows returning solvent sensitivity (compare traces a_2 and b_2 in Fig. $5B$).

We considered that the recovering solvent sensitivity of secondary activation seen in Fig. $5B$ might depend on some hidden solvent-sensitive process occuring during the longer (400 μs) interval at holding potential. For example, if fast voltage-sensitive gating processes were sufficient to close the sodium channels, then the slower channel dehydration step might be undetectable in the tail currents. However, the increasing percentage of nonhydrated channels at increasing interpulse intervals would slow the subsequent activation process towards the control rate seen during primary activation. This hypothesis predicts that hyperosmolar media should slow the "hidden" deactivation rate for channel dehydration, thus increasing the interpulse interval required to reestablish the control primary activation rate.
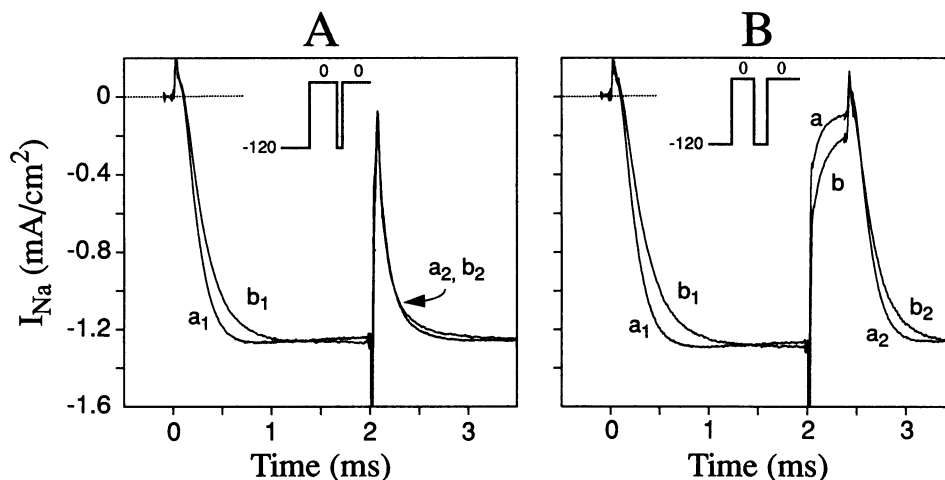

FIGURE 5   Effects of hyperosmolar sucrose perfusion on primary activation (traces a_1 and b_1) and secondary activation (traces a_2 and b_2) for two different interpulse intervals. Axon pretreated with chloramine-T to remove fast inactivation. Trace a is the control in isosmolar internal perfusate; trace b is after exposure to 0.9 osmol/kg sucrose medium. Traces b were scaled to match the control trace at 2 ms. Test potential 0 mV; holding potential -120 mV. (A) Interpulse interval is 50 μs. All traces overlie during secondary activation despite the kinetic differences evident during primary activation. (B) Interpulse interval is 400 μs. After this longer interpulse interval, secondary activation shows some recovery towards the solvent-sensitivity evident during primary activation. Note the clipping of the tail currents in these scaled records. All data from axon 900807.

Recovery of secondary activation rate towards primary activation kinetics can be quantified, for any interpulse interval, as:

$$\text{recovery} = (\Delta t 1/2_{\max} - \Delta t 1/2)/\Delta t 1/2_{\max},$$

where the change in half activation times between primary and secondary activation is "$\Delta t 1/2$" and where the maximum change in half activation times (observed for a 50 μs interpulse interval) is "$\Delta t 1/2_{\max}$." Comparing recovery rates by this method for the data of Fig. 5 B, we found that recovery in 400 μs was 77% for trace a_2 in isosmolar perfusate, whereas recovery was only 66% for trace b_2. As predicted, recovery towards the kinetics of primary activation is slower in hyperosmolar perfusates. However, we have already seen that IgOFF is unaffected by hyperosmolar media (see Fig. 4 B). Thus, the slowing of recovery towards primary activation kinetics cannot result from changes in the rates of voltage-sensitive processes. This slower recovery must reflect some hidden solvent-sensitive process, such as that hypothesized above.

DISCUSSION

Our results have made clear that osmotic stress affects the kinetics of some, but not all, of the processes involved in activation and deactivation of sodium channels (cf. D_2O effects, Alicata et al., 1990). In axons with intact fast inactivation, both activation and inactivation are slowed by hyperosmolar media, whereas peak conductance is suppressed in relation to the applied osmotic stress (see Fig. 1). After removal of fast inactivation with chloramine-T (Wang et al., 1985) internal perfusion with hyperosmolar media demonstrates that, although solvent-sensitive processes affect the rate of primary activation, the rates of deactivation and secondary activation are insensitive to osmotic stress. Thus, osmotic stress, like D_2O (see Alicata et al., 1990), discriminates two alternative pathways for channel activation. We shall argue that these pathways reflect parallel voltage-sensitive and solvent-sensitive gating processes, which are nevertheless "coupled" such that: (a) primary activation is initiated by gating charge movements in the channel walls. These charge movements open the voltage-sensitive gate(s) although the channel remains nonconducting due to the closed (nonhydrated) state of the channel interior. However, gating charge movements destabilize this nonhydrated conformation, triggering hydration of the channel and transition into its final ion-conducting state. (b) Deactivation results from rapid gating charge movements which directly close the voltage-sensitive gate(s). These charge movements additionally destabilize the hydrated channel conformation, leading

to subsequent dehydration of the channel interior. (c) Secondary activation occurs when channels have been deactivated by the voltage-sensitive gate(s) but have not yet lost their hydrated conformation. They can then reopen with rapid kinetics which are not affected by the solvent-sensitive gating mechanism.

Comparison of squid and crayfish data

The principal focus of this study has been on the kinetic effects of osmotic stress on sodium channels. However, the conclusions suggested above incorporate concepts introduced by Zimmerberg et al. (1990) for delayed rectifier potassium channels in squid axons. We have therefore repeated the key findings of that study on crayfish axon sodium channels. We note that increased solution osmolarity decreases macroscopic sodium conductance (see Table 1). Quantitatively consistent results were obtained using osmotic agents (sucrose and formamide) which would be expected to have very different modes of interaction with binding sites in the ion-permeation pathway. Our results thus support the conclusion of Zimmerberg et al. (1990) that the decrease in macroscopic conductance does not result from "blocking" the conducting path for sodium ions. Furthermore the current-voltage curves obtained in these experiments indicate no changes in sodium channel reversal potential after changes in solution osmolarity. Just as in the delayed rectifier channels, we found that the osmotically induced decrease in macroscopic conductance is not affected by changes in test potential across the range −20 to 40 mV (Fig. 3). The lack of effect of high osmolar solutions on gating currents (Fig. 4) is further evidence that the reduction in macroscopic conductance results

TABLE 1 Computed volume changes

Agent	π_1	π_2	G_2/G_1^*	$\Delta V^{\dagger}$	Inactivation
	osmol/kg	osmol/kg		Å^3	
Sucrose	0.44	0.82	0.77	1,157	removed
	0.44	0.88	0.85	632	removed
	0.44	0.82	0.91	405	removed
	0.44	0.82	0.89	525	removed
	0.44	0.88	0.79	934	intact
	0.43	1.23	0.59	1,114	removed
	0.44	1.30	0.60	1,025	intact
Formamide	0.44	1.70	0.75	402	intact
	0.44	2.90	0.49	507	intact
	0.44	2.90	0.44	582	intact
				728 ± 297	
				($n = 10$)	

*Ratio of peak conductance at 0 mV; †calculated from Eq. 4, Zimmerburg et al. (1990).

from primarily voltage-insensitive mechanisms. Finally, the changes in conductance arise without change in external solution conductivity. Thus, we can dismiss both channel "block" and conductivity changes as sources of the observed effects.

Neither our study nor that of Zimmerberg et al. (1990) have included the single channel data which could provide conclusive demonstration that osmotically induced changes in macroscopic conductance arise from changes in probability of channel opening, rather than from changes in single channel conductance. Two kinds of osmotically induced changes seem possible at the microscopic level: (a) graded changes in single channel conductance might occur in all channels within the population or, (b) channels might be forced into a subconductance state by increase in osmotic stress, as occurs with the voltage dependent anion channel (VDAC) studied by Zimmerberg and Parsegian (1986). The first mechanism suggests that the solute inaccessible space should increase with increasing solution osmolarity; we see no signs of such an effect (see Table 1). The second mechanism suggests that macroscopic conductance would asymptote at the fractional conductance of the subconductance state; again we see no signs of such behavior in our axons. Presently available evidence thus continues to favor the analysis presented by Zimmerberg et al. (1990).

The solute inaccessible volume of sodium channels

Zimmerberg and Parsegian (1986) point out that equiosmolar changes of both internal and external media are required for appropriate thermodynamic definition of equilibrium conditions (see also Zimmerberg et al., 1990). We recognize that this necessary condition was not achieved in the work presented here. On the other hand, our previous results for both formamide (Alicata et al., 1989) and D_2O (Alicata et al., 1990) demonstrate that quantitatively similar kinetic data may be obtained with only internal presentation of the modified solvent. Furthermore, both our analysis (see Appendix) and that of Zimmerberg et al. (1990) make clear that volume estimates should be obtained from changes in conductance at test potentials > 20 mV (see Ruben et al., 1990) where the voltage-sensitive gating mechanism is close to full saturation. However, as shown in Fig. 3, the fractional suppression of macroscopic conductance is essentially independent of voltage for test potentials > -20 mV. Our estimate, that the solute inaccessible volume in sodium channels (~ 700 Å^3, see Table 1) is around half that calculated for delayed rectifier channels ($\sim 1,350$ Å^3, Zimmerberg et al., 1990), should nevertheless be

confirmed by additional work avoiding the limitations noted here.

Table 1 provides two additional findings: first, we note the similar estimates of solute inaccessible volume obtained from both sucrose and formamide solutions. Formamide is a small molecule (45 D), with a dielectric constant of 84, which is widely used as an ionizing solvent. We had considered that formamide might penetrate the solute excluded space, perhaps directly competing with water molecules as an alternative solvent. However, the similarity in osmotic volume estimates between formamide and sucrose data (see Table 1) suggests that formamide remains a purely osmotic agent at these concentrations. Second, we note the essentially identical estimates of osmotic volume obtained from axons with intact fast inactivation (690 Å^3 $\pm$ 273, $n = 5$) and from axons with fast inactivation removed (766 Å^3 $\pm$ 347, $n = 5$).

The kinetic effects of hyperosmolar perfusates

Additional insight into the mechanisms of sodium channel gating is offered by our finding that only some of the processes involved in activation, deactivation, and fast inactivation of sodium channels are affected by hyperosmolar perfusates. We explore the implications of these results in reference to simplified models in which the multiple voltage-sensitive steps of the activation process have been collapsed into a single voltage-sensitive transition (see Appendix 1 of Zimmerberg et al., 1990). Whereas such simplifications distort quantitative predictions of axon kinetics, qualitative changes become considerably easier to understand.

Fig. 6 presents model simulations which explore three different ways in which voltage-sensitive and solvent-sensitive gating mechanisms could be linked together: (a) they could be so tightly coupled (for example, by an allosteric mechanism) that they would necessarily occur in fixed sequence (scheme 1); (b) they could exist as independent parallel gating mechanisms (scheme 2); or, (c) these parallel gating mechanisms could be loosely coupled (for example, by weak electrostatic interactions as in scheme 3). At positive potentials, where the voltage-sensitive transition approaches saturation, the equilibrium effects of osmotic stress will be entirely determined by the solvent-sensitive transition. Hence, all models predict identical equilibrium effects of hyperosmolar solutions at these potentials (see also Zimmerberg et al., 1990). On the other hand, these models predict qualitatively very different *kinetic* responses to osmotic stress. The parameters of the voltage-sensitive (V_s) and solvent-sensitive (S_s) transitions are identical in each model. Voltage-sensitive reaction rates were calcu-
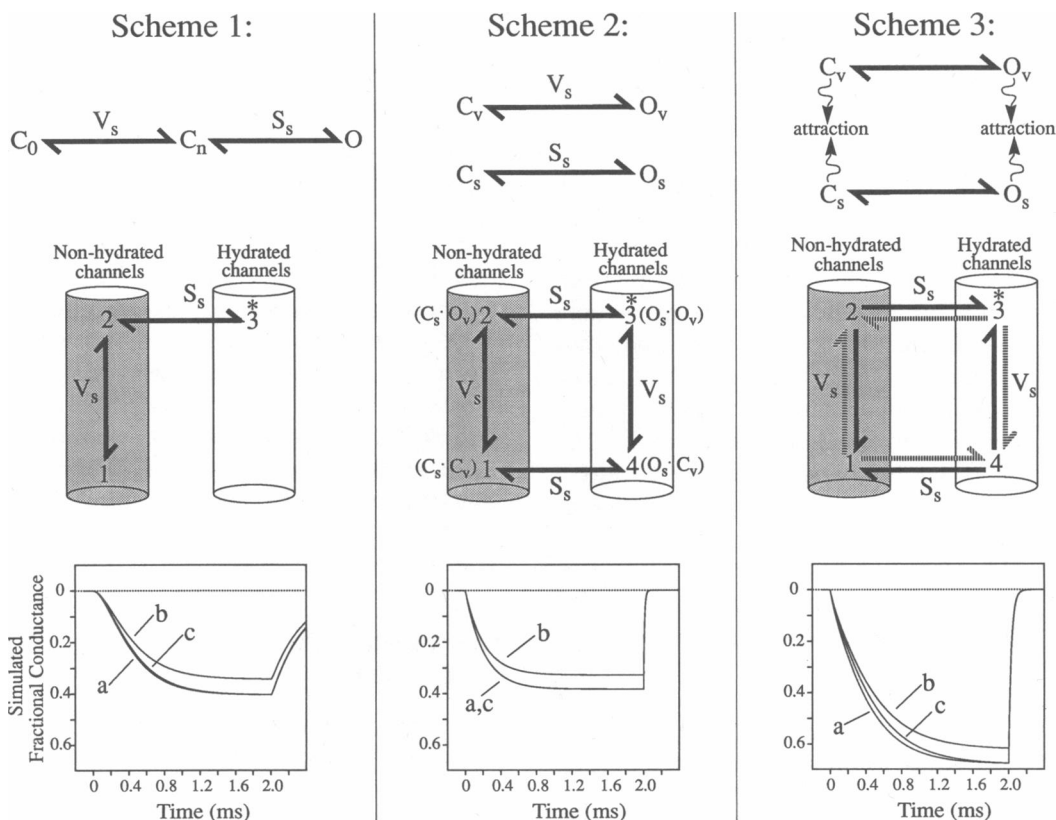
FIGURE 6 Simulated kinetic and equilibrium effects of osmotic stress. We compare predictions from three different models for the relationship between voltage-sensitive (V_s) and solvent-sensitive (S_s) transitions. (*Upper panels*) A conventional kinetic diagram. (*Middle panels*) V_s as vertical and S_s steps as horizontal, and differentiate transitions occuring in hydrated and dehydrated channel configurations. (*Lower panels*) Simulated experimental records, where traces *a* simulate control records in isosmolar perfusate (0.45 osmol/kg), traces *b* show predicted effects of exposure to 0.9 osmol/kg internal perfusate and traces *c* show traces *b* rescaled to match control peak conductance. V_s and S_s parameters (see below) were the same for each model; assumptions of the modeling process are detailed in the Appendix. All simulations are for steps from -120 mV to 0 mV. V_s parameters (all models): $w_a = 21$; $w_b = 23$; $x = 0.5$; $z = 2$. S_s parameters (all models): $w_a = w_b = 21$; $x = 0.95$; $\Delta v = 1,000$ Å^3. Coupling parameters (scheme 3 model only): $W_1 = -0.25$; $W_2 = 0.25$; $W_3 = -1$; $W_4 = 1$.

lated using the modified equations introduced by Bezanilla et al. (1982). Solvent-sensitive rates were obtained by a simple extension of Eyring rate theory (Glasstone et al., 1941), see Appendix.

The sequential model

Because our results have shown that osmotic stress slows channel opening without noticeable effect on gating currents, the simplified sequential model used here (see Fig. 6, scheme 1) places the solvent-sensitive transition as the final opening step. This scheme 1 model is presented both as a linear three-state sequence (Fig. 6, upper panel) and in an equivalent form (Fig. 6, middle panel) where voltage-sensitive transitions (V_s) are shown vertical whereas solvent-sensitive transitions (S_s) are horizontal. Where the solvent-sensitive transition between state 2 and the open state (3*) is slow enough to

significantly retard channel opening, then this process must also retard tail current deactivation (from 3* to 2). *Thus, the scheme 1 model predicts that tail currents will be slow and solvent-sensitive,* in direct contrast to the data presented here (see Figs. 1 *C*, 1 *F*, 2 *A*, 2 *B*, and 5), as well as to the lack of effect of D_2O on tail current kinetics (Schauf and Bullock, 1982; Alicata et al., 1990). Furthermore the scheme 1 model necessarily requires the voltage-sensitive transition (2,1) to occur only in nonhydrated channels (as if channel hydration "immobilizes" the gating charges by some unspecified mechanism). Hence, this model requires that IgOFF should be similarly slowed, because voltage-sensitive transitions would be "immobilized" in each channel until the channel loses its waters of hydration.

This sequential model cannot be salvaged by changes in kinetic parameters. If the solvent-sensitive step is made fast enough that it no longer limits deactivation

rate, then activation rate also ceases to be affected by solvent changes. The relative lack of effect of osmotic stress on deactivation rate was also noted by Zimmerberg et al. (1990) in delayed rectifier potassium channels. We therefore suggest that similar discrepancies between prediction and experimental data will be found for all models in which voltage-sensitive transitions are considered as necessarily preceding a final voltage-insensitive (but solvent-sensitive) step into the open state. We question both models in which the voltage-sensitive reactions are considered as parallel and independent (Zagotta and Aldrich, 1990a,b; Keynes, 1990), and models in which a sequence of voltage-sensitive steps was assumed (Scanley et al., 1990; Solc and Aldrich, 1990). Both types of models can be reduced to the simple sequential form shown in Fig. 6, scheme 1.

The parallel independent model

The parallel model considered by Zimmerberg et al (1990) as an alternative to scheme 1, can again be represented in two equivalent forms (see Fig. 6, scheme 2). In this simple parallel system both the voltage-sensitive and solvent-sensitive processes must reach their "open" states (O_v and O_s) before the channel becomes conducting. When this model is presented in its alternative format (Fig. 6, middle panel), we note that the rate constants must remain symmetrical regardless of changes in channel hydration or position of the gating "particles." The solvent-sensitive gate modulates maximum conductance by controlling the fraction of "openable channels" (i.e., the fraction of channels moving between states 3* and 4). This fraction will be altered only by changes in osmotic stress. Thus, it is an inevitable property of this scheme 2 model that applied potential cannot affect opening or closing of the solvent-sensitive gates. Necessarily, therefore, *this parallel model predicts that the kinetics of both activation and deactivation will be insensitive to osmotic stress.* By contrast, in our experimental data, we find that primary activation is slowed by exposure to hyperosmolar perfusates (see Figs. 1 *B*, 1 *E*, 2 *C*, and 5). A similar osmotic slowing was seen by Zimmerberg et al. (1990) in delayed rectifier channels. Because D_2O substitution also slows primary activation rate (Meves, 1974; Schauf and Bullock, 1979; Alicata et al., 1990) the simple scheme 2 model is clearly insufficient as a predictor of solvent-sensitive channel kinetics.

The coupled parallel model

The evidence summarized above appears to rule out both the linear sequential (scheme 1) and parallel independent (scheme 2) models from further serious consideration. We have therefore investigated a model in which parallel voltage-sensitive and solvent-sensitive

gates are presumed to be coupled, such that voltage-sensitive gating processes necessarily precede solvent-sensitive changes in channel hydration (during both activation and deactivation of sodium channels). This model is shown in Fig. 6, scheme 3, where solid arrows are used to indicate the unidirectional processes which become favored (see middle panel) by the coupling resulting from the "attractions" between voltage-sensitive and solvent-sensitive open and closed states (see top panel). Comparing the 2,3* and 1,4 transitions in this coupled model, we see that the open state (3*) is favored during depolarization, whereas state 1 is favored in resting channels. (Equivalent changes in the voltage-sensitive transitions are required to maintain microscopic reversibility.) We shall demonstrate that the general predictions of this kinetic approach are consistent with our data, before considering possible physical mechanisms which might underlie such a kinetic scheme.

Evidence from activation kinetics

The activation kinetics predicted by this model are essentially those of linear sequential models (derived primarily from activation data). During activation, this model is formally equivalent to the models proposed by Zagotta and Aldrich (1990a,b), Keynes (1990), and Solc and Aldrich (1990). The scheme 3 model is also consistent with our data showing that hyperosmolar media slow channel opening without noticeably affecting the kinetics of IgON.

Evidence from deactivation kinetics

Here the coupled parallel model departs radically from the predictions of linear sequential models, by suggesting that channel closings during deactivation result primarily from voltage-sensitive, rather than solvent-sensitive, gating mechanisms. The model conforms to the results shown in Fig. 2 where no solvent-sensitive phase of tail current kinetics was detected. However, "hidden" solvent-sensitive gating is predicted during prolonged returns to holding potential, as channels progress from state 4 to state 1 after the initial gating transition from state 3* to state 4. Solvent-sensitive slowing of this 4 to 1 transition explains our observed slower return to primary activation kinetics during secondary activation in presence of hyperosmolar perfusate (see Fig. 5 *B*).

Evidence from model simulations

The bottom panels in Fig. 6 show computer simulations of 2 ms depolarizing steps from −120 mV holding potential to 0 mV test potential in normal (0.45 osmol/ kg) and hyperosmolar (0.9 osmol/kg) solutions, for each of the three models considered above. The assumptions required to specify effects of osmotic stress on the rates for the solvent-sensitive transition are presented in the

Appendix. All parameters were identical for each model, except that the coupling energies required to achieve sequentiality in activation and deactivation steps were explicitly included only in the scheme 3 model (see Appendix). For each simulation, trace a shows the response in normal medium, trace b is the response in hyperosmolar medium (note the reduced peak conductance), and trace c shows the hyperosmolar response rescaled to control peak magnitude to emphasize any kinetic differences between normal and hyperosmolar traces. As predicted above, the scheme 1 model shows very slow tail currents, the scheme 2 model shows faster deactivation but no slowing of activation in hyperosmolar medium, whereas the scheme 3 model shows both fast deactivation and osmotic slowing of activation rate. However, there are some interesting additional results which may be noted in these simulations. The slowing of activation is small (only $\Delta t1/2 = 16$ μs) in the scheme 1 simulation. By contrast the coupling included in scheme 3 enhances the slowing of activation ($\Delta t1/2 = 33$ μs) towards that seen in Figs. 1 B, 1 E, 2 C, and 5. Furthermore, this coupling considerably increases the maximum sodium conductance seen in model 3 as compared to models 1 and 2 (to $\sim 70\%$ from $\sim 40\%$ of the total channel population). Nevertheless, the effect of osmotic stress in all three models remains well described by a simple Boltzmann equation (see Appendix).

Zimmerberg et al. (1990) point out that coupling between the voltage-sensitive and solvent-sensitive steps (even where no explicit coupling energy is included in the model, as in scheme 1) must necessarily shift the voltage midpoint for the overall activation process. Thus, they conclude that the open state of the solvent-sensitive transition must be minimally absorbent, because they detect no statistically significant shift in the apparent midpoints of their G(V) curves. It is thus particularly noteworthy that the individual coupling energies used in our scheme 3 model are extremely small, no $> 1/20$th of kT. We find that these energies generate shifts in the apparent midpoint voltage of ~ 2 mV for a twofold change in osmolarity, which is within the range (not > 5 mV) specified by Zimmerberg et al. (1990). Nevertheless, the properties of the overall system are changed such as to produce a relatively absorbent open state under depolarized conditions.

A biophysical basis for the coupled parallel model

Parsegian (1982) has pointed out that strong hydration forces, which must be overcome to exclude water from between closely approaching biological macromolecules (see also Rau et al., 1984), may be approximately balanced by forces of attraction which include not only van der Waal's forces but also electrostatic components from detailed charge interactions as well as an entropic component from the high order of hydration waters. Because coulombic forces are strengthened by the exit of polarizable water molecules, "on-or-off" behavior can be predicted through relatively minor variations in these large competing forces. (It would be interesting to know whether the voltage-insensitive "gating" behavior of the synthetic channel protein studied by Oiki et al [1988], see also Montal [1990], is affected by osmotic stress).

The principal conclusion suggested by the kinetic data presented here is that some form of coupling must exist between structurally parallel voltage-sensitive and solvent-sensitive gating mechanisms. We propose that movements of charged gating particles within the walls of voltage-gated channels can affect the balance of forces described above, so as to favor either hydration or dehydration of the channel interior depending on gating particle position. Hence, the voltage-insensitive hydration process becomes functionally coupled to the voltage-sensitive mechanisms of channel gating. However, the form of coupling used for the simulations presented here (see Appendix) was arbitrarily selected and is not the only mechanism compatible with our data. More extensive work will be required to fully characterize the nature and extent of the coupling forces between channel hydration and each of the multiple parallel gating particles presumably present within a tetrameric sodium channel molecule.

Finally, we note the most general conclusion which emerges from the studies carried out by Parsegian and his co-workers: functionally significant conformational changes in protein molecules are likely to alter the number of polar and polarizable residues exposed to the aqueous medium, thus altering the required number of waters of solvation. Such conformational changes necessarily acquire an osmotic work component, which may be rate limiting even under physiological conditions (Parsegian, 1991; Colombo et al., 1991) because the additional water molecules must be extracted from osmotic solution. Our study supports both this general conclusion and the previous work (Zimmerberg and Parsegian, 1986; Zimmerberg et al., 1990) indicating that this concept is applicable to some, but not all, of the conformational changes involved in ion channel gating.

APPENDIX

Kinetics of the solvent-sensitive process

Following Eyring rate theory (Glasstone et al., 1941), where W_π is the osmotic work (defined as the product of osmotic pressure, π, and

change of solute excluded channel volume, Δv, see Zimmerberg and Parsegian [1986]), and where increase in osmotic work reduces the rate of channel opening, then forward $(k_{a,b})$ and backward $(k_{b,a})$ rates are given by:

$$k_{a,b} = (kT/h) \cdot \exp(W_a - \omega_a - x(W_\pi)/kT) \qquad (1)$$

$$k_{b,a} = (kT/h) \cdot \exp(W_b - \omega_b + (1-x)(W_\pi)/kT) \qquad (2)$$

where kT and h have their usual significance, where barrier heights (ω_a and ω_b) are expressed in the same units as kT, where x reflects the fraction of the distance between wells A and B at which the barrier occurs, and where W_a and W_b are coupling forces (expressed as changes in barrier height, see below). We see no a priori reason why the opposing forces affecting channel opening and closing probabilities (see text) should be equally balanced in the absence of osmotic stress, hence ω_a and ω_b are not necessarily equal when $W_\pi = 0$. However, we have assumed the barrier position to be highly asymmetric ($x = 0.95$) to reflect a near total exclusion of solute from its inaccessible interior volume represented here as "well B."

Equilibrium effects of osmotic stress in the coupled model

If A is the fraction of channels in state A and $B = (1 - A)$, and where W_A is the sum of the nonosmotic energy terms, such that:

$$W_A = \omega_a - \omega_b + W_b - W_a, \qquad (3)$$

then the Boltzmann relationship for a solvent-sensitive transition can be written as:

$$B/A = \exp - [W_A + (W_\pi/kT)] \qquad (4)$$

Furthermore, at saturating positive potentials all voltage-sensitive gates can be presumed to be in their "open" configuration. Thus, in our models only the coupling inherent in the 2,3* reaction needs to be considered in evaluating effects of osmotic stress on the equilibrium distribution of conducting channels. Thus, if O_1 and O_2 are the fractions of conducting channels at osmotic pressures π_1 and π_2, where the ratio:

$$r = [O_2/(1 - O_2)]/[O_1/(1 - O_1)], \qquad (5)$$

then:

$$\log_n(r) = - (W_{A_{2,3}} + (\pi_2 - \pi_1)\Delta v/kT). \qquad (6)$$

This simple relationship accurately predicts the simulated conductance changes (at saturating positive potentials) for all three models considered here. Note that $W_{A_{2,3}}$ is -1.25 for our scheme 3 simulations, i.e., $\sim 1/20$th of kT (see Fig. 6).

Coupling between voltage-sensitive and solvent-sensitive processes

Following general principles of Eyring rate theory, interactions across a given state can be specified as resulting from an appropriate change in the well energy for that state. Thus, for the hypothesis that gating particles and hydration waters might mutually attract one another in the open (hydrated) state of the channel, this attraction can be described as a lowering of the well energy for state 3*. If this well is reduced by an amount $-W_3$, then the two reactions leading out of this state will be slowed proportionately. Similarly, a repulsive coupling force can be introduced as an increase in well energy (as for state 2),

where the reactions leading out of this state will be proportionately accelerated. If coupling is specified in this manner, all models will necessarily obey the requirements of microscopic reversibility regardless of the symmetry, or lack of symmetry, of the coupling energies. Furthermore, because change of well energy changes the barrier heights seen from that well, it becomes apparent that the coupling energies should be expressed in the same dimensional units as the barrier energies and as kT (see Eq. 3).

Voltage-sensitive reaction rates can then be calculated using the modified rate equations introduced by Bezanilla et al. (1982) and used by Stimers et al. (1985, 1987) and Rayner and Starkus (1989). Thus, k_α and k_β are:

$$k_\alpha = (kT/h) \cdot \exp(W_a - w_a + ezxV/kT) \qquad (7)$$

$$k_\beta = (kT/h) \cdot \exp(W_b - w_b - ez(1 - x)V/kT), \qquad (8)$$

where w is the height of the energy barrier (in kT units) as seen from well a or b, respectively, e is the electronic charge, z is the effective valence for the transition, V is applied membrane potential, and all other symbols are as previously defined.

As a result of the general nature of this formulation, we can now specify the condition for independence of the solvent-sensitive reaction from voltage sensor movements as:

$$W_1 + W_3 = W_2 + W_4 \qquad (9)$$

Where coupling energies are chosen which do *not* meet this condition, the solvent-sensitive reaction will be differentially affected by voltage sensor position. The coupling energies for the scheme 3 model presented here were selected following the arbitrary assumption that W_1 and W_3 would be negative where W_2 and W_4 are positive. For this coupling system, the largest kinetic effects of osmotic stress were obtained when the interaction energies were higher for the hydrated channel conformation than for nonhydrated states.

In this combined voltage-sensitive and solvent-sensitive model, we have found it simplest to convert all energy units to equivalent units. Hence, the coupling energies shown in the legend for Fig. 6 are given in millivolts. Substituting Eqs. 1, 2, 7, and 8 into the model formulations shown in Fig. 6 then permits the kinetic behavior of these models to be examined using standard iterative simulation methods (see Methods, also Alicata et al., 1990).

REFERENCES

Alicata, D. A., M. D. Rayner, and J. G. Starkus. 1989. Osmotic and pharmacological effects of formamide on capacity current, gating

current, and sodium current in crayfish giant axons. *Biophys. J.* 55:347–353.

Alicata, D. A., M. D. Rayner, and J. G. Starkus. 1990. Sodium channel activation mechanisms: insights from deuterium oxide substitution. *Biophys. J.* 57:745–758.

Bezanilla, F., R. E. Taylor, and J. M. Fernandez. 1982. Distribution and kinetics of membrane dielectric polarization. 1. Long-term inactivation of gating currents. *J. Gen. Physiol.* 79:21–40.

Colombo, M. F., D. C. Rau, and V. A. Parsegian. 1991. Regulation of hemoglobin activity by water molecules. *Biophys. J.* 59:611a. (Abstr.)

Glasstone, S., K. J. Laidler, and H. Eyring. 1941. The Theory of Rate Processes. McGraw-Hill Inc., New York. 522–599.

Hahin, R. 1988. Removal of inactivation causes time-invariant sodium current decays. *J. Gen. Physiol.* 92:331–350.

Heggeness, S. T., and J. G. Starkus. 1986. Saxitoxin and tetrodotoxin. Electrostatic effects on sodium channel gating in crayfish giant axons. *Biophys. J.* 49:629–643.

Keynes, R. D. 1990. A series-parallel model of the voltage-gated sodium channel. *Proc. R. Soc. Lond. B. Biol. Sci.* 240:425–432.

Ludeman, L. C. 1986. Fundamentals of digital signal processing. Harper and Row, New York. 330 pp.

Meves, H. 1974. The effect of holding potential on the asymmetry currents in squid giant axons. *J. Physiol. (Lond.).* 243:847–867.

Montal, M. 1990. Channel protein engineering: an approach to the identification of molecular determinants of function in voltage-gated and ligand-regulated channel proteins. *Ion Channels.* 2:1–31.

Oiki, S., W. Danho, and M. Montal. 1988. Channel protein engineering: synthetic 22-mer peptide from the primary structure of the voltage-sensitive sodium channel forms ionic channels in lipid bilayers. *Proc. Natl. Acad. Sci. USA.* 85:2393–2397.

Parsegian, V. A. 1982. Physical forces due to the state of water bounding biological materials: some lessons for the design of colloidal systems. *Adv. Colloidal Interfacial Sci.* 16:49–56.

Parsegian, V. A. 1991. Forces for a better physics of bio-molecular organization. *Biophys. J.* 59:566a. (Abstr.)

Oxford, Gerry S. 1981. Some kinetic and steady-state properties of sodium channels after removal of inactivation. *J. Gen. Physiol.* 77:1–22.

Rau, D. C., B. Lee, and V. A. Parsegian. 1984. Measurement of the repulsive force between polyelectrolyte molecules in ionic solution: hydration forces between parallel DNA double helices. *Proc. Natl. Acad. Sci. USA.* 81:2621–2625.

Rayner, M. D., and J. G. Starkus. 1989. The steady-state distribution of gating charge in crayfish giant axons. *Biophys. J.* 55:1–19.

Rayner, M. D., and J. G. Starkus. 1991. Voltage-sensitive and solvent-sensitive processes in ion channel gating: effects of osmotic stress on crayfish sodium channels. *Physiologist.* 34:105a. (Abstr.)

Ruben, P. C., J. G. Starkus, and M. D. Rayner. 1990. Holding potential affects the apparent voltage-sensitivity of sodium channel activation in crayfish giant axons. *Biophys. J.* 58:1169–1181.

Scanley, B. E., D. A. Hanck, T. Chay, and H. A. Fozzard. 1990. Kinetic analysis of single sodium channels from canine cardiac purkinje cells. *J. Gen. Physiol.* 95:411–437.

Schauf, C. L., and J. O. Bullock. 1979. Modifications of sodium channel gating in *Myxicola* giant axons by deuterium oxide, temperature, and internal cations. *Biophys. J.* 27:193–208.

Schauf, C. L., and J. O. Bullock. 1980. Solvent substitution as a probe of channel gating in *Myxicola*. Differential effects of D_2O on some components of membrane conductance. *Biophys. J.* 30:295–306.

Schauf, C. L., and J. O. Bullock. 1982. Solvent substitution as a probe of channel gating in *Myxicola*. Effects of D_2O on kinetic properties of drugs that occlude channels. *Biophys. J.* 37:441–452.

Shrager, P. 1974. Ionic conductance changes in voltage clamped crayfish axons at low pH. *J. Gen. Physiol.* 64:666–690.

Shrager, P., J. G. Starkus, M-V. C. Lo, and C. Peracchia. 1983. The periaxonal space of crayfish giant axons. *J. Gen. Physiol.* 82:221–244.

Solc, C. K., and R. W. Aldrich. 1990. Gating of single non-*Shaker* A-type potassium channels in larval *Drosophila* neurons. *J. Gen. Physiol.* 96:135–165.

Starkus, J. G., S. T. Heggeness, and M. D. Rayner. 1984. Kinetic analysis of sodium channel block by internal methylene blue in pronased crayfish giant axons. *Biophys. J.* 46:205–218.

Starkus, J. G., M. D. Rayner, P. C. Ruben, and D. A. Alicata. 1991. Voltage-sensitive and solvent-sensitive processes in ion channel gating: effects of hyperosmolar media on activation and deactivation kinetics in sodium channels. *Biophys. J.* 59:71a. (Abstr.)

Stimers, J. R., F. Bezanilla, and R. E. Taylor. 1985. Sodium channel activation in the squid giant axon. Steady state properties. *J. Gen. Physiol.* 85:65–82.

Stimers, J. R., F. Bezanilla, and R. E. Taylor. 1987. Sodium channel gating currents. Origin of the rising phase. *J. Gen. Physiol.* 89:521–540.

Wang, G. K., M. S. Brodwick, and D. C. Eaton. 1985. Removal of sodium channel inactivation in squid axon by the oxidant chloramine-T. *J. Gen. Physiol.* 86:289–302.

Zagotta, W. N., and R. W. Aldrich. 1990a. Voltage-dependent gating of *Shaker* A-type potassium channels in *Drosophila* muscle. *J. Gen. Physiol.* 95:29–60.

Zagotta, W. N., and R. W. Aldrich. 1990b. Alterations in activation gating of single *Shaker* A-type potassium channels by Sh^5 mutation. *J. Neurosci.* 10:1799–1810.

Zimmerberg, J., and V. A. Parsegian. 1986. Polymer inaccessible volume changes during opening and closing of a voltage-dependent ionic channel. *Nature (Lond.).* 323:36–39.

Zimmerberg, J., F. Bezanilla, and V. A. Parsegian. 1990. Solute inaccessible aqueous volume changes during opening of the potassium channel of the squid giant axon. *Biophys. J.* 57:1049–1064.